Supporting Information for "A new mechanism for mineralizing systems based on cnoidal wave instabilities"

Chong Liu[1], Victor M. Calo[2], Lisa Tannock[4], Klaus Regenauer-Lieb[3,4],

Manman Hu[1]

[1]Department of Civil Engineering, The University of Hong Kong, Hong Kong, China

[2]School of Electrical Engineering, Computing and Mathematical Sciences, Curtin University, Perth, WA 6845, Australia

[3]WA School of Mines: Minerals, Energy and Chemical Engineering, Curtin, Bentley, WA 6102, Australia

[4]School of Minerals and Energy Resources Engineering, UNSW, Sydney, NSW 2052, Australia

Contents of this file

1. Text S1

2. Figures S1 to S2

Corresponding author: Manman Hu, Department of Civil Engineering, The Univerity of Hong Kong, Haking Wong Building, Pokfulam Road, Hong Kong, China. (mmhu@hku.hk)

September 14, 2023, 8:56am

Introduction

The following supplementary materials are included below:

- Text S1: Methodology for a physical model of cnoidal waves in poromechanics

- Figure S1: Varied perturbation distributions in the center of the compressive specimen for different stress peaks by adjusting the parameter s in Eq. (S11).

- Figure S2: Evolution of perturbation at five iteration steps for the five peaks case by the adaptive stabilized finite element method (ASFEM).

Text S1. Methodology for a physical model of cnoidal waves in poromechanics

We derive a 1-D formulation for cnoidal waves based on the general theory of plasticity (Hill, 1962) and poromechanics (Coussy, 2004). Hill's approach simplifies a generalized 2-D problem into an equivalent 1-D one. Poromechanis enables us to study the fundamental competition between fluid flow and mechanical deformation. In analogy to the stress state of materials in compressive geosystems, we consider a homogeneous material of length H under a constant compression at its boundary in the x direction, as Figure 1 shows in the main manuscript. We assume a perturbation p'_n greater than the yield stress p'_y exists in the center of the compressed specimen. The periodic boundary conditions are imposed at the two ends, mimicking one unit in a geological setting. In addition, we assume all material properties are constant for mathematical simplicity, such as solid viscosity and permeability.

We solve this poromechanics problem under the framework of overstress viscoplasticity by Perzyna (1966). The effective stress in the specimen is $p = p' + p_f$ as defined in Terzaghi's theory, where p is the mean stress with positive in compression and p_f is the pore pressure. The momentum balance equation reads as

$$\nabla p' = -\nabla p_f \tag{S1}$$

For the conservation of mass, we should consider the internal mass transfer between the solid and fluid phases because the chemical reaction is likely to occur in the diagenetic window. The general reaction formation for the dissolution/precipitation can be expressed as

$$AB_{(s)} \rightleftharpoons A_{(s)} + B_{(aq)} \tag{S2}$$

September 14, 2023, 8:56am

:

As for the quartz veins formation in the diagenetic reaction, AB and A are smectite and illite, and B denotes the aqueous quartz.

In a binary solid-fluid mixture system, we define the partial mass densities $\rho^s := \phi^s \rho_s$ and $\rho^f := \phi^f \rho_f$ for the solid and fluid phases, respectively, with ϕ^s and ϕ^f the volume fraction of the solid and fluid phase, ρ_s and ρ_f the solid skeleton and fluid density. Note that $\phi^s + \phi^f = 1$ in the bi-phasic setting. The mass balance equations for both solid and fluid phases read as

$$\begin{aligned} \frac{\mathrm{d}\rho^s}{\mathrm{d}t} + \rho^s \nabla \cdot v &= -j \\ \frac{\mathrm{d}\rho^f}{\mathrm{d}t} + \rho^f \nabla \cdot v_f &= j \end{aligned} \tag{S3}$$

where j is the internal mass transfer by the diagenetic reaction in the fluid-rock interaction, v and v_f are the solid and fluid velocities, respectively. We drop the subscript 's' for the solid velocity since it is the reference velocity.

Adding Eq. (S3) together and noting that the bi-phasic setting of $\phi^s + \phi^f = 1$, we have

$$\nabla \cdot v + \nabla \cdot \bar{v} = j \left(\frac{1}{\rho_f} - \frac{1}{\rho_s} \right) \tag{S4}$$

where $\bar{v} := \phi^f(v_f - v)$ is the Darcy flux, denoting the relative volumetric rate of fluid flow to the matrix. We have the following relationship between the relative rate and the compaction rate and Darcy's law for laminar flow

$$\bar{v} = -\frac{k}{\mu_f} \nabla p_f \tag{S5}$$

where k is the permeability, μ_f is the fluid viscosity.

Furthermore, we define the volumetric strain rate for the solid $\dot{\varepsilon}_v := \nabla \cdot v$ in Eq. (S4), which contains two components: a reversible elastic part $\dot{\varepsilon}_v^e$ and an irreversible (visco)plastic part $\dot{\varepsilon}_v^p$ (Perzyna, 1966). The former $\dot{\varepsilon}_v^e$ is related to the mean effective

stress rate by the elastic rate constitutive equation, whereas a typical power law rheology expresses the latter $\dot{\varepsilon}_v^p$ (Kohlstedt et al., 1995). Therefore, the total volumetric strain rate can be written as

$$\dot{\varepsilon}_v = \dot{\varepsilon}_v^e + \dot{\varepsilon}_v^p = -\frac{\dot{p}'}{K^e} - \dot{\varepsilon}_n \left[\frac{\bar{p}}{\bar{p}_n}\right]^m \tag{S6}$$

where p' and $\dot{p}'$ are the effective stress and its rate, K^e is the elastic bulk modulus, $\dot{\varepsilon}_n$ is the reference loading strain rate corresponding to the perturbation stress p'_n, $\bar{p} := p' - p'_Y$ and $\bar{p}_n := p'_n - p'_Y$ are the effective and reference overstresses in which p'_Y is the yield stress, and m is the rate sensitivity exponent and has a value above 1 for geomaterials in general. The negative signs are consistent with positive stresses in compression.

Introducing the following dimensionless parameters:

$$\sigma := \frac{\bar{p}}{\bar{p}_n}, \quad \tau := \frac{kK^e}{\mu_f H^2}t, \quad x^* := \frac{x}{H}, \tag{S7}$$

And assuming the rate of fluid production j follows an Arrhenius relationship with a dependence on the mean pressure of the activation enthalpy, we have pressure-enhance precipitation form for j as

$$j = -Ae^{\beta\sigma} \tag{S8}$$

where A is a coefficient, and β is a chemo-mechanical parameter representing the interaction between the mass transfer rate and the external loading.

Substituting Eq. (S5)–(S8) into Eq. (S4), we have the dimensionless formulation as

$$\frac{\partial \sigma}{\partial \tau} = \frac{\partial^2 \sigma}{\partial x^{*2}} - \lambda \sigma^m + \eta e^{\beta\sigma}, \tag{S9}$$

in which $\lambda := \frac{\mu_f \dot{\varepsilon}_n}{k\bar{p}_n}H^2$ and $\eta := \frac{A\mu_f H^2}{k\bar{p}_n}\left(\frac{1}{\rho_f} - \frac{1}{\rho_s}\right)$. Dropping the left-hand side term of the asterisk and only considering the steady-state case in our study, we obtain the final

dimensionless formulation for static-state cnoidal waves:

$$\frac{\partial^2 \sigma}{\partial x^{*2}} - \lambda \sigma^m + \eta e^{\beta \sigma} = 0 \tag{S10}$$

We solve the above equation using the adaptive stabilized finite element method (AS-FEM), to capture the stress concentration phenomenon. This is because the ASFEM can overcome the spurious oscillations in the classical FEM for this high nonlinear problem. The detailed discretization and formulation for the ASFEM refer to Cier, Poulet, Rojas, Veveakis, and Calo (2021). We perform our simulations in FEniCS and set the material properties as $\eta = 4.54 \times 10^{-9}$ and $\beta = 10$. We assume that the guess perturbation u_{IG} is located in the center of the specimen as

$$u_{IG} = \frac{2.5 \sin x\pi}{\sin(\pi/2)} \exp\left(\frac{-0.5(x - 0.5)^2}{s^2}\right) \tag{S11}$$

where s is a constant adjusting the size of perturbation and the symbol u denotes $\sigma - 1$. This is because this replacement allows transferring the inhomogeneous ($\sigma = 1$) into homogeneous ($u = 0$) Dirichlet boundary conditions (Cier et al., 2021). We adopt this representation, although we assign the periodic boundary conditions at the two ends of the specimen. The specimen is initially divided into 100 elements and it can be adaptively refined with the peak evolution.

References

Cier, R. J., Poulet, T., Rojas, S., Veveakis, M., & Calo, V. M. (2021). Automatically adaptive stabilized finite elements and continuation analysis for compaction banding in geomaterials. *International Journal for Numerical Methods in Engineering*, *122*(21), 6234–6252.

Coussy, O. (2004). *Poromechanics*. John Wiley & Sons.

Hill, R. (1962). Acceleration waves in solids. *Journal of the Mechanics and Physics of Solids*, *10*(1), 1–16.

Kohlstedt, D., Evans, B., & Mackwell, S. (1995). Strength of the lithosphere: Constraints imposed by laboratory experiments. *Journal of Geophysical Research: Solid Earth*, *100*(B9), 17587–17602.

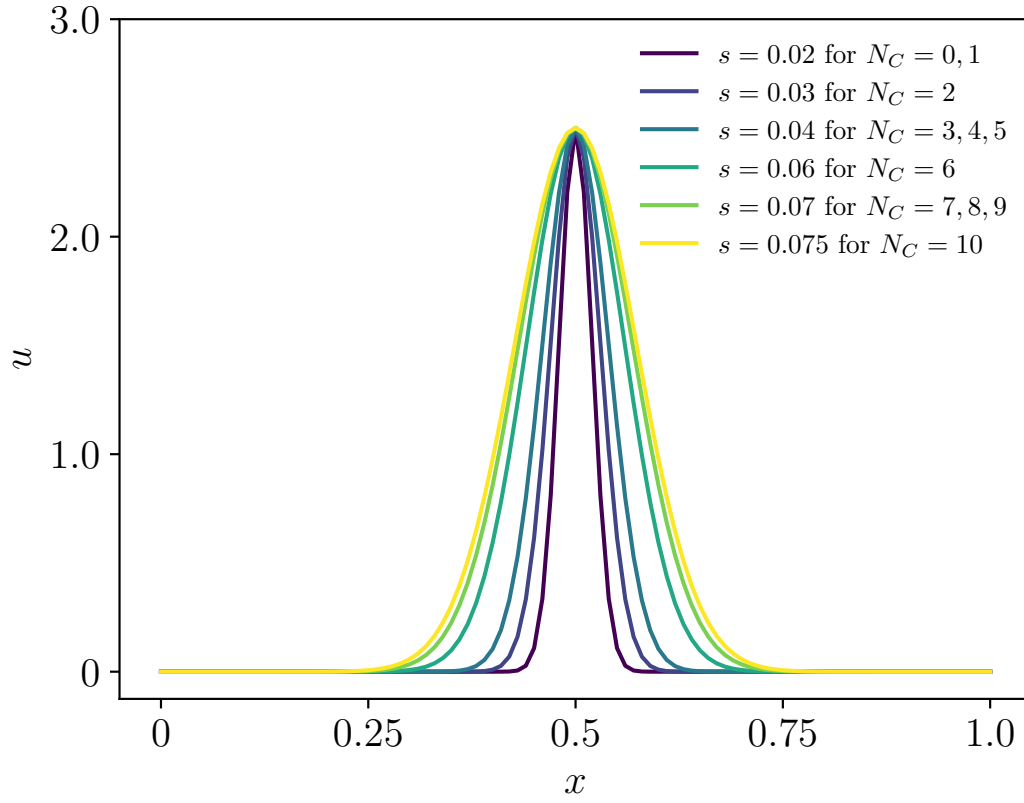Perzyna, P. (1966). Fundamental problems in viscoplasticity. *Advances in Applied Mechanics*, *9*, 243–377.

Figure S1. Varied perturbation distributions in the center of the compressive specimen for different stress peaks by adjusting the parameter s in Eq. (S11).
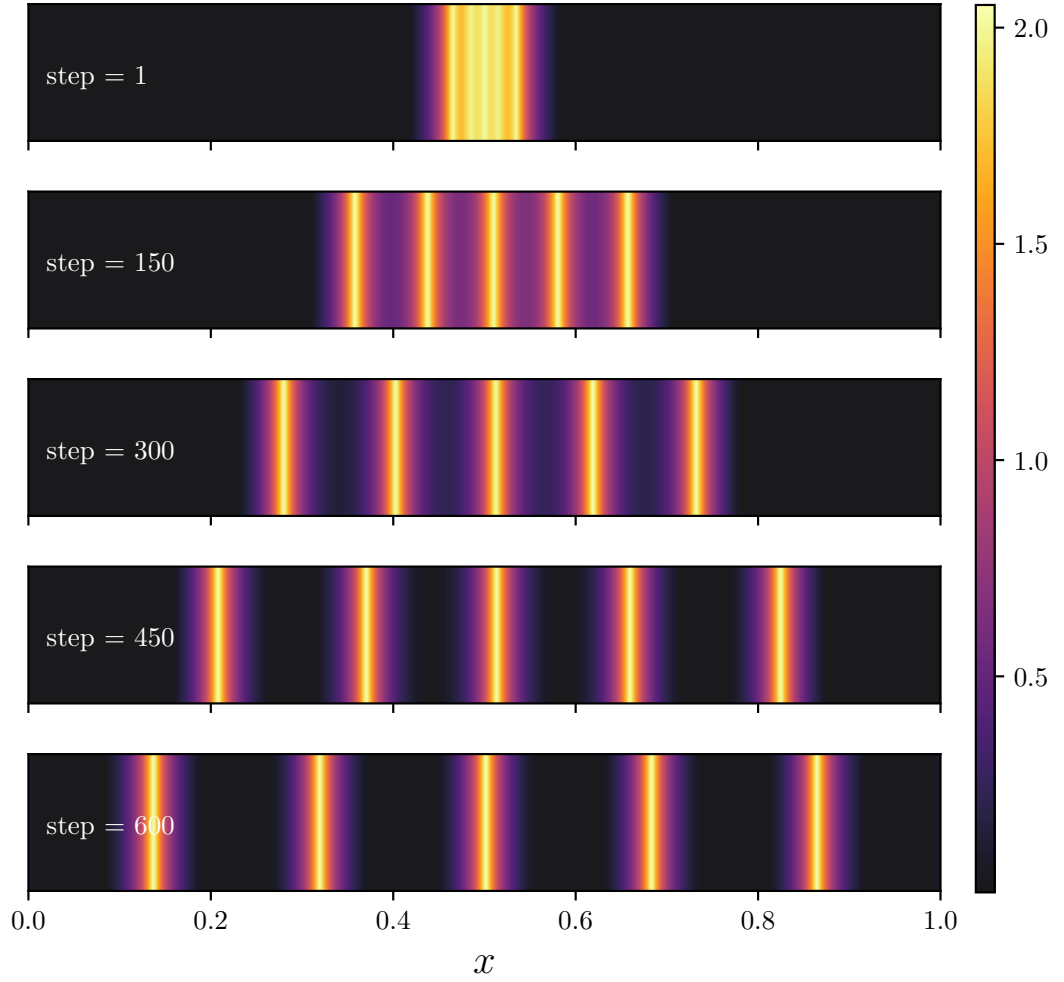
Figure S2. Evolution of perturbation at five iteration steps for the five peaks case by the adaptively stabilized finite element method (ASFEM).